Local Structure of Framework Iron in Fe-Substituted Al-Mordenites by Fe K Edge XAFS

6 AUTHORS, INCLUDING:

Hirofumi Aritani
Saitama Institute of Technology
40 PUBLICATIONS   **699** CITATIONS

SEE PROFILE

Tsunehiro Tanaka
Kyoto University
318 PUBLICATIONS   **6,004** CITATIONS

SEE PROFILE

Local Structure of Framework Iron in Fe-Substituted Al-Mordenites by Fe K Edge XAFS

Hirofumi Aritani,*,† Shuichi Nishimura,† Masato Tamai,† Takashi Yamamoto,‡ Tsunehiro Tanaka,‡ and Atsushi Nakahira†

Faculty of Engineering and Design, Kyoto Institute of Technology, Sakyo-ku, Kyoto 606-8585, Japan, and Department of Molecular Engineering, Graduate School of Engineering, Kyoto University, Kyoto 606-8501, Japan

The Fe-substituted Al-mordenites (Fe-MOR) with several Fe ratios were synthesized, and the detailed structure was obtained by means of Al K edge XANES and Fe K edge XAFS. From the results of the N_2-adsorption isotherm, the Fe-substituted mordenites with an Fe/(Fe + Al) ratio as high as 75 mol % have a high crystallinity and appropriate micropore. The completely substituted mordenite (Fe100MOR) shows low pore volume and mordenite crystallinity. The Al K edge XANES results show the smaller effect of structural change around Al ions by Fe (25 mol %) substitution. Fe K edge XAFS results indicate existence of tetrahedral Fe ions into the mordenite framework in all the Fe ratios. The local structure around the Fe^{3+} ions is quite different from that around the Fe-modified mordenites. The Fe−O distance increases with an increase in Fe content. This suggests the distortion of the zeolite framework in the local structure of the mordenites. It is concluded that the stable structure around the Fe^{3+} ions in the Fe-substituted mordenites is brought up to about 75 mol % in the Fe ratio.

Introduction

H-mordenite (without modification of transitional metals) is an active catalyst for selective catalytic reduction (SCR) of NO[1−3] or isomerization of alkanes such as *n*-butane.[4] This catalytic activity is based on strong acidity,[5] and the acidity is controllable by dealumination. It is reported that the dealuminated mordenite also shows a high activity for SCR of NO with CH_4.[6] The mordenite is a comfortable material to control the catalytic activity of SCR of NO by appropriate treatment. To enhance the activity and selectivity, the addition of transitional-metal cations onto mordenites has been studied by means of several preparation methods.

Fe-modified zeolites have been reported as being used for selective oxidation or as NO_x-SCR catalysts.[7] For instance, Fe-modified MFI zeolite shows high activity for SCR of NO[8,9] or N_2O[10−12] with hydrocarbons. Feng et al.[13] reported that over-exchanged Fe-MFI shows more durable activity for SCR of NO_x than Cu-MFI. The SCR activity and durability of Fe-MFI in the presence of water vapor were studied by Chen et al.[14] Marturano et al.[15,16] have presented the relation between the detailed Fe structure in over-exchanged Fe-MFI and deNO$_x$ activity.

In recent years, Fe-incorporated MFI zeolites have been applied to not only SCR of NO_x but also selective oxidation catalysts. Ribera et al.[17] reported that Fe-substituted MFI prepared by hydrothermal synthesis shows high activity for selective oxidation of benzene to phenol. Panov et al.[18] overviewed the Fe-incorporated MFI catalysts and proposed the generation of active oxygen species on Fe−ZSM-5 surfaces. It is noted that the incorporation of Fe ions in the zeolite framework brings about not only the stabilization of active Fe species but also the generation of unique activity for

* To whom correspondence should be addressed. Present address: Department of Applied Chemistry, Saitama Institute of Technology, Okabe, Saitama 369-0293, Japan.
† Kyoto Institute of Technology.
‡ Kyoto University.
(1) Miro, E. E.; Imoberdoff, G.; Vassallo, J.; Petunchi, J. O. *Appl. Catal., B* **1999**, *22*, 305.
(2) Ribotta, A.; Lezcano, M.; Kurgansky, M.; Miró, E.; Lombardo, E.; Petunchi, J.; Moreaux, C.; Dereppe, J. M. *Catal. Lett.* **1997**, *49*, 77.
(3) Chung, S. Y.; Oh, S.-H.; Kim, M. H.; Nam, I.-S.; Kim, Y. G. *Catal. Today* **1999**, *54*, 521.
(4) Asuquo, R. A.; Eder-Mirth, G.; Seshan, K.; Pieterse, J. A. Z.; Lercher, J. A. *J. Catal.* **1997**, *168*, 292.
(5) Makarova, M. A.; Wilson, A. E.; Liemt, B. J.; Mesters, C. M. A. M.; de Winter, A. W.; Williams, C. *J. Catal.* **1997**, *172*, 170.
(6) Lezcano, M.; Ribotta, A.; Miró, E.; Lombardo, E.; Petunchi, J.; Moreaux, C.; Dereppe, J. M. *J. Catal.* **1997**, *168*, 511.
(7) Chen, H.-Y.; Wang, X.; Sachtler, W. M. H. *Appl. Catal., A* **2000**, *194*, 159.
(8) Iwamoto, M.; Yahiro, H. *Catal. Today* **1994**, *22*, 5.
(9) Voskoboinikov, T. V.; Chen, H.-Y.; Sachtler, W. M. H. *Appl. Catal., B* **1998**, *19*, 279.
(10) Rauscher, M.; Kesore, K.; Mönnig, R.; Schwieger, W.; Tissler, A.; Turek, T. *Appl. Catal., A* **1999**, *184*, 249.
(11) Centi, G.; Vazzana, F. *Catal. Today* **1999**, *53*, 683.
(12) Pophal, C.; Yogo, T.; Tanabe, K.; Segawa, K. *Catal. Lett.* **1997**, *44*, 271.
(13) Feng, X.; Hall, W. K. *J. Catal.* **1997**, *166*, 368.
(14) Chen, H.-Y.; Sachtler, W. M. H. *Catal. Today* **1998**, *42*, 73.
(15) Marturano, P.; Kogelbauer, A.; Prins, R. *J. Catal.* **2000**, *190*, 460.
(16) Marturano, P.; Drozdová, L.; Kogelbauer, A.; Prins, R. *J. Catal.* **2000**, *192*, 236.
(17) Ribera, A.; Arends, I. W. C. E.; de Vries, S.; Pérez-Ramírez, J.; Sheldon, R. A. *J. Catal.* **2000**, *195*, 287.
(18) Panov, G. I.; Uriarte, A. K.; Rodkin, M. A.; Sobolev, V. I. *Catal. Today* **1998**, *41*, 365.

selective oxidation of hydrocarbons. With regard to Fe-substituted mordenites (Fe-MOR), however, only a few studies have been reported. Isomorphous substitution of Fe for Al into the zeolites by several preparation methods has been studied. In recent years, Fe-incorporated metallosilicates (ferrisilicate) with several types of zeolites (such as MFI, beta, FER, and MCM-22) have been reported by several workers[19−24] and it have been applied to the catalysts with redox activity.[25,26] Wu et al.[27] found that Fe^{3+}-substituted mordenites can be synthesized under template-free conditions. As a result, Fe-substituted Al-mordenite materials can be expected to act as appropriate catalysts for selective oxidation and SCR of NO with high and durable activity. In our previous study,[28] Fe-MOR with high crystallinity could be synthesized hydrothermally by using the tetraethyl-ammonium (TEA) template, and the Fe ratio (Fe/(Fe + Al)) in the Fe-mordenites could be controlled in the range of 0−100 mol % Fe. In this study, however, the results of characterization were supplied only by means of XRD and SEM. For the application of the catalyst material, detailed evaluation of local structure around Fe ions in Fe-MOR with several Fe ratios is required. In addition, the difference between substituted and modified (ion-exchanged or impregnated) mordenites needs to be clarified. In this study, Fe K edge XAFS was applied to the characterization of incorporated Fe^{3+} in Fe-MOR materials to clarify the detailed local structure around Fe ions in the mordenite framework. In addition, the XANES study at Al K edge was added to clarify the local structure of each atom in the zeolite framework.

Experimental Section

The Fe-MOR samples are prepared by the method described in a separate paper.[28] In brief, Fe-mordenites with several Fe/(Fe + Al) ratios were synthesized hydrothermally at 423 K for more than 7 days. The $Na_2O-Fe_2O_3$(and/or Al_2O_3)$-SiO_2-H_2O$ system and TEA were used as the template. After all, the optimum gel composition, 7.7 Na_2O: 2 TEA: $(0.4 − x)$ Al_2O_3: x Fe_2O_3: 23 SiO_2: 700 H_2O $(0 \le x \le 0.4)$, gives the highest Fe-MOR crystallinity. Finally, the dried gel was calcined at 873 K for 6 h. In this paper, the materials were denoted as FeNMOR in which N possesses the molar ratio of Fe (N = (Fe/(Fe + Al)) × 100%). The composition of each atom in the Fe-MOR samples obtained by elemental analysis is shown in Table 1. The composition ratios of $SiO_2/(Al_2O_3 + Fe_2O_3)$ on the Fe-MOR samples were in the range of 13.0−13.6. For Fe-free mordenite (denoted as Al-MOR), the ratio of SiO_2/Al_2O_3 was 14.1. As a reference material, NaAl-mordenite (JRC-Z-M15, SiO_2/Al_2O_3 = 15.4, denoted as NaAl-MOR) was applied to compare the structural information.

Table 1. Composition of Fe-MOR Samples[a]

sample	composition (wt % (mol %))			
	SiO_2	Al_2O_3	Fe_2O_3	Na_2O
Al-MOR	85.1 (89.0)	10.3 (6.3)	0.0 (0.0)	4.6 (4.7)
Fe25MOR	83.3 (88.8)	7.6 (4.8)	4.7 (1.9)	4.4 (4.5)
Fe50MOR	81.4 (88.2)	4.8 (3.0)	8.7 (3.5)	4.1 (4.3)
Fe75MOR	80.3 (88.3)	2.4 (1.5)	12.6 (5.2)	4.7 (5.0)
Fe100MOR	78.3 (86.9)	0.2 (0.2)	15.6 (6.5)	5.9 (6.4)

[a] Synthesized in this study.

The elemental analysis was carried out by X-ray fluorescence spectroscopy (Phillips PW1480). The isotherms for N_2 adsorption at 77 K were measured in a Belsorp 18SP (Japan-Bell Co.). Typically, 0.1 g of powdered sample was evacuated at 573 K before the adsorption measurements. The values of specific surface area and the pore volume were evaluated by means of Langmuir theory and t-plot, respectively.

The Fe K edge XAFS (XANES and EXAFS) spectra of the samples were collected by a facility of the BL-7C station at the Photon Factory in the National Laboratory for High Energy Physics (KEK-PF), with 2.5 GeV of ring energy and 200−350 mA of stored current, in a transmission mode at room temperature. The ionization chambers filled with N_2 (as I_0) and Ar(25%)−N_2 (as I) gases were used as transmitted beam detectors, and ex situ samples were set between these detectors. The photon source was monochromatized by means of Si(111) double-crystal monochromator (d = 3.135 51 Å). A channel-cut chamber line and a 1 mm slit were used for the elimination of harmonics. Computational analyses for the XAFS spectra were performed with the FACOM M1800 computer system at the Data Processing Center of Kyoto University. Each spectrum was normalized to the height of the McMaster curve which is an approximation of absorption by a free atom after removal of the contribution from absorption other than the K edge absorption, as described elsewhere.[29,30] The k^3-weighted EXAFS spectra were obtained from normalized EXAFS spectra, and Fourier transformations were performed within the range of $\Delta k = 4−15$ Å^{-1} without any phase shift correction. Curve-fitting analyses were performed within $\Delta k = 4−12$ Å^{-1} with the empirical parameters extracted from well-crystallized $FeAl_2O_4$ (spinel) for Fe−O shell in the range of $\Delta R = 1.2−1.9$ Å.

The Al K edge XANES spectra were collected on the BL-7A station[31,32] of the soft X-ray beam line at the UVSOR facility, in the Institute for Molecular Science, Okazaki, Japan (with a ring energy of 750 MeV and stored current of 120−220 mA). Each sample was mounted on carbon tape and then attached to a beryllium−copper dynode as the first stage of the electron multiplier placed in a vacuum chamber. After the chamber was evacuated ($<2.0 \times 10^{-7}$ Torr), the spectrum was measured in the total electron yield mode at room temperature, using a KTP (KTiOPO_4)(011) double-crystal monochromator ($2d$ = 1.0954 nm). At the Al K edge, the resolution of the photon energy was less than 0.5 eV. As described in the above section, low-energy secondary electrons constitute a significant fraction of the spectra in this mode. Because the penetration range is less than 38 nm into the bulk, the XANES spectra reflect the structure of the samples in "near-surface region".[33,34] The

(19) Zecchina, A.; Geogaldo, F.; Lamberti, C.; Bordiga, S.; Turnes Palomino, G.; Otero Areán, C. *Catal. Lett.* **1996**, *42*, 25.

(20) Matsubayashi, N.; Shumada, H.; Imamura, M.; Sato, T.; Okabe, K.; Yoshimura, Y.; Nishijima, A. *Catal. Today* **1996**, *29*, 273.

(21) Bordiga, S.; Buzzoni, R.; Geobaldo, F.; Lamberti, C.; Giamello, E.; Zecchina, A.; Leofanti, G.; Petrini, G.; Tozzola, G.; Vlaic, G. *J. Catal.* **1996**, *158*, 486.

(22) Borade, R. B.; Clearfield, A. *Chem. Commun.* **1996**, *1996*, 2267.

(23) Wu, P.; Lin, H.; Komatsu, T.; Yashima, T. *Chem. Commun.* **1997**, *1997*, 663.

(24) Tuel, A.; Arcon, I.; Millet, J. M. M. *J. Chem. Soc., Faraday Trans.* **1998**, *94*, 3501.

(25) Brabec, L.; Jeschke, M.; Kilk, R.; Nováková, J.; Kubelková, L.; Meusinger, J. *Appl. Catal., A* **1998**, *170*, 105.

(26) Uddin, M. A.; Komatsu, T.; Yashima, T. *J. Chem. Soc., Faraday Trans.* **1995**, *91*, 3275.

(27) Wu, P.; Komatsu, T.; Yashima, T. *Microporous Mesoporous Mater.* **1998**, *20*, 139.

(28) Nakahira, A.; Nishimura, S.; Aritani, H.; Yamamoto, T.; Ueda, S. *J. Mater. Sci.* **2001**, *36* (8), 1885.

(29) Tanaka, T.; Yamashita, H.; Tsuchitani, R.; Funabiki, T.; Yoshida, S. *J. Chem. Soc., Faraday Trans. 1* **1988**, *84*, 2987.

(30) Yamamoto, T.; Tanaka, T.; Takenaka, S.; Yoshida, S.; Onari, T.; Takahashi, Y.; Kosaka, T.; Hasegawa, S.; Kudo, M. *J. Phys. Chem.* **1999**, *103*, 2385.

(31) Murata, T.; Matsukawa, T.; Naoe, T.; Horigome, S.; Matsudo, O.; Matanabe, M. *Rev. Sci. Instrum.* **1992**, *63*, 1309.

(32) Kinoshita, T.; Takata, Y.; Matsukawa, T.; Aritani, H.; Matsuo, S.; Yamamoto, T.; Takahashi, M.; Yoshida, H.; Yoshida, T.; Ufuktepe, Y.; Nath, K. G.; Kimura, S.; Kitajima, Y. *J. Synchrotron Radiat.* **1998**, *5*, 726.

(33) Elam, W. T.; Kirkland, J. P.; Neiser, R. A.; Wolf, P. D. *Phys. Rev. B* **1995**, *38*, 1.

(34) Erbil, A.; Cargill, G. S., III; Frahm, R.; Boehme, R. F. *Phys. Rev. B* **1988**, *37*, 2450.
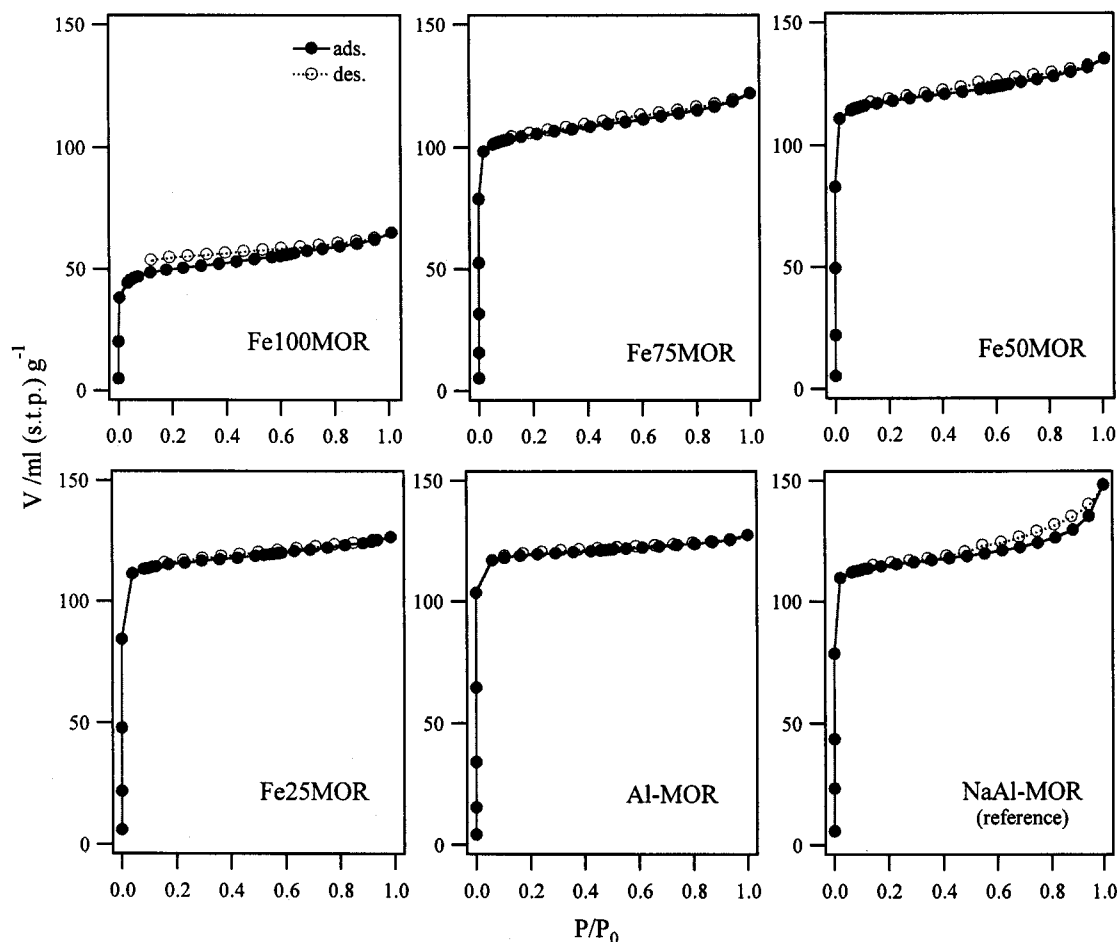
Figure 1. N_2-adsorption isotherms of Fe-MOR samples at 77 K.

photon energy was calibrated at the Al K edge (1559 eV) by using an aluminum metal foil.

Results and Discussion

1. Isotherm of N_2 Adsorption. The results of characterization mainly by using XRD and SEM were described in previous papers.[28,35] In summary, the Fe-MOR materials synthesized hydrothermally have a mordenite structure with high crystallinity; however, the crystallinity of Fe100MOR was lower than those of other Fe-MOR samples.

To investigate the micropore structure in the mordenite samples, the N_2-adsorption method was employed. The isotherms at 77 K are shown in Figure 1. In the whole samples, the characteristic steep is not seen, indicating that ordered meso- or macropores are absent. In the initial step less than $P/P_0 = 0.05$, adsorption steep due to mordenite micropores should be overlapped to adsorption background. With respect to the volumes adsorbed, the Fe-MOR and Al-MOR samples are almost similar to the NaAl-MOR reference with the exception of Fe100MOR. For this sample, the volume is quite less than the others. To obtain a detailed parameter, the specific surface area and pore volume were obtained by means of Langmuir theory and t-plot, respectively. The results are shown in Table 2. In both surface area (A) and pore volume (V_p), the values of Al-MOR, Fe25MOR,

Table 2. Specific Surface Area[a] (A) and Evaluated Pore Volume[b] (V_p) of Fe-MOR Samples

sample	A (m^2 g^{-1})	V_p (μL g^{-1})
Al-MOR	526	177
Fe25MOR	513	163
Fe50MOR	524	167
Fe75MOR	470	143
Fe100MOR	226	60
Na-MOR (reference)	512	163

[a] Evaluated by means of Langmuir-type model. [b] Evaluated by means of t-plot.

and Fe50MOR are almost similar to that of NaAl-MOR in the range of 512–526 m^2 g^{-1}. For Fe75MOR, the values become a little smaller. In the case of Fe100MOR, the values are much lower than those of the other samples, supporting the above results. From these results, it is summarized that the Fe-substituted mordenites with high Fe ratio up to 75 mol % have high crystallinity of mordenite structure and appropriate micropore structure. On the other hand, the crystallinity of Fe100MOR is very low. It suggests that the complete substitution by the Fe^{3+} ions in Al^{3+}-mordenite brings about the weak stability of the zeolite framework.

2. Al K Edge XANES. The Al K edge XANES was applied to investigate the local structure of the zeolite framework.[36] The XANES spectra of Al-MOR, Fe25MOR, and reference Al-compounds are shown in Figure 2.

(35) Nakahira, A.; Nishimura, S.; Ueda, S. *J. Soc. Mater. Sci., Jpn.* **2000**, *49*, 887.

(36) van Bokhoven, J. A.; Sambe, H.; Ramaker, D. E.; Konings-berger, D. C. *J. Phys. Chem. B* **1999**, *103*, 7557.
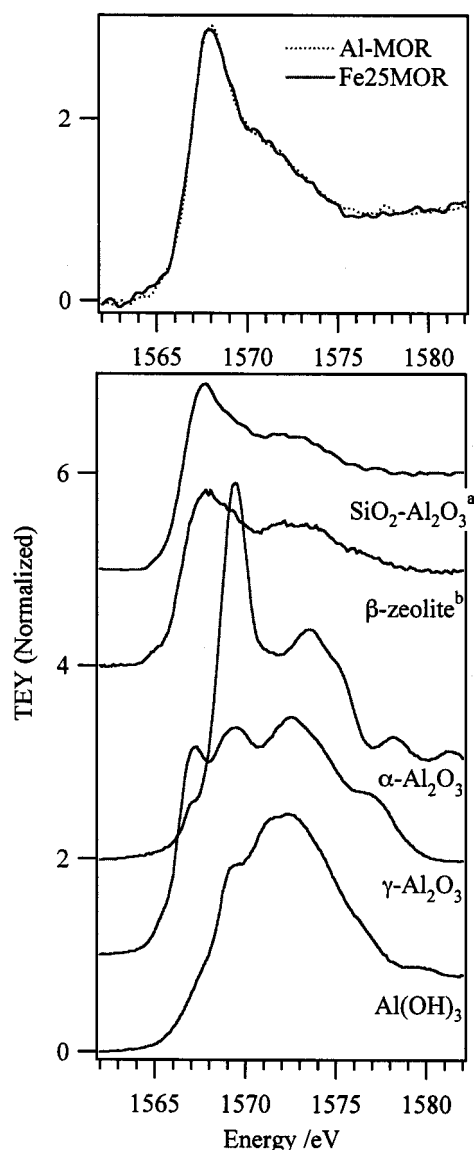
Figure 2. Al K edge XANES spectra of mordenite samples (top) and reference Al compounds (bottom) ([a]amorphous silica−alumina (JRC-SAL-2, 13.8 wt % Al_2O_3), [b]beta-zeolite (JRC-H-BEA25, SiO_2/Al_2O_3 = 25)).

Because of the Al content being too small, the spectra of Fe50MOR, Fe75MOR, and Fe100MOR could not be obtained clearly. Recently, Shimizu et al.[37] reported the Al K edge XANES study of several Al^{3+} compounds. They suggested that the two XANES peaks in lower and higher energy in near-edge (1565−1570 eV) were due to Al−O_4 tetrahedra and Al−O_6, respectively. For the reference compounds in our study, β-zeolite (JRC-H-BEA25) and amorphous silica−alumina (JRC-SAL-2) show the peak at around 1568 eV, supporting the existence of Al−O_4 tetrahedra. The XANES spectrum of rock-salt α-Al_2O_3 shows a prominent peak at 1569.5 eV. In the case of Al(OH)$_3$-containing distorted octahedra, a shoulder peak at ca. 1569 eV can be seen. For the XANES spectrum of γ-Al_2O_3-containing tetrahedra

and octahedra, the peaks are seen at ca. 1568 and 1569.5 eV. The evaluation of the Al local structure by means of near-edge XANES peaks is conventional when Al ions exist as tetrahedra and/or octahedra, as reported recently by Kato et al.[38] In addition, the peak position of the samples is in good agreement with that of the results reported in the reference. Thus, the assignment to tetrahedral or octahedral Al ion is definite. The Al ions in the mordenite samples (Al- and Fe-MOR) should consist of T_d tetrahedra. The XANES spectra of these samples are shown in Figure 2. The spectra of Al-MOR and Fe25MOR are similar to each other, indicating the similar structure around Al ions. In addition, the peak centered at 1568 eV is due to the tetrahedral Al structure. Thus, it is summarized that the Al ion in the Al-MOR framework is stabilized as tetrahedra, and the structural change is not seen by the substitution of the Fe ion in the case of Fe25MOR.

3. Fe K Edge XAFS. Figure 3 shows the Fe K edge XANES of Fe-MOR samples, Fe-modified mordenites (Fe/MOR), and reference Fe compounds. To compare the structures of Fe-modified samples, we prepared two samples, i.e., Fe ion-exchanged mordenite (Fe 1.1 wt %, denoted as Fe/MOR(iex)) and Fe-impregnated mordenite (Fe 6.8 wt %, denoted as Fe/MOR(imp)) samples. In the case of Fe ion-exchanged or impregnated mordenite (Fe/MOR) samples, the XANES spectra are almost the same as FeOOH and/or Fe(OH)$_3$, suggesting the formation of distorted octahedra. The XANES spectra of Fe-MOR in the whole Fe ratio are different from those of Fe/MOR. In the case of Fe-MOR samples, the XANES show a pre-edge peak with large intensity. It suggests the existence of Fe^{3+} ions with tetrahedral and/or highly distorted octahedral structure. With respect to the XANES feature of Fe-MOR, the absorption in the postedge region (7140−7150 eV) increases with an increase in Fe ratio. The XANES spectrum of $NaFeO_2$ ($NaCrS_2$-type structure, highly distorted Fe−O_6 octahedra) shows significant pre-peak and resonance peaks (in the postedge region) which are similar to that of Fe100MOR. Thus, it can be suggested that Fe ions in the Fe-MOR samples consist of tetrahedral and highly distorted octahedral structure, and the octahedral component increases with increase in Fe ratio.

EXAFS analysis was carried out to obtain the structural parameters of Fe ions in the zeolite framework. The k^3-weighted EXAFS oscillation waves of Fe-MOR samples are shown in Figure 4. The oscillation waves of all the Fe-MOR samples are almost identical and each consists of almost a single sine wave. The oscillation wave of Fe/MOR(imp) is similar not to that of Fe-MOR but to that of Fe_2O_3. This indicates that local structure around Fe^{3+} ions in Fe/MOR is quite different from that in Fe-MOR. The EXAFS oscillation waves of Fe-MORs are also different from that of $NaFeO_2$, while the XANES spectra are similar to each other. It indicates that the local structure of Fe in Fe-MOR is different from that in $NaFeO_2$ with highly distorted octahedra.

Figure 5 shows the Fourier transformed (FT) EXAFS of Fe-MOR and other samples. In the case of reference Fe compounds (FeOOH, $NaFeO_2$, Fe_2O_3, and Fe(OH)$_3$), more than two FT peaks can be seen due to Fe−O and

(37) Shimizu, K.; Kato, Y.; Yoshida, T.; Yoshida, H.; Satsuma, A.; Hattori, T. *Chem. Commun.* **1999**, 1681.

(38) Kato, Y.; Shimizu, K.; Matsushita, N.; Yoshida, T.; Yoshida, H.; Satsuma, A.; Hattori, T. *Phys. Chem. Chem. Phys.* **2001**, *3*, 1925.
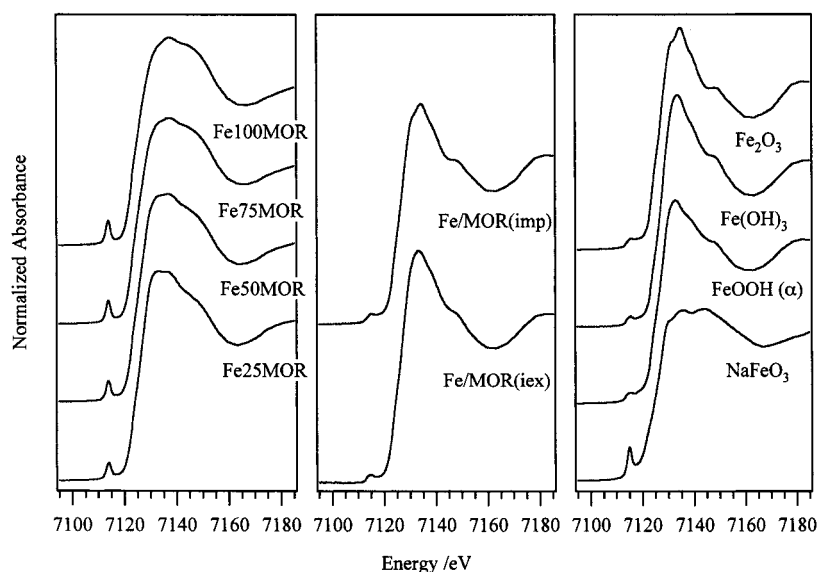
Figure 3. Fe K edge XANES spectra of Fe-substituted (left) and Fe-modified (center) mordenite samples and reference Fe compounds (right).
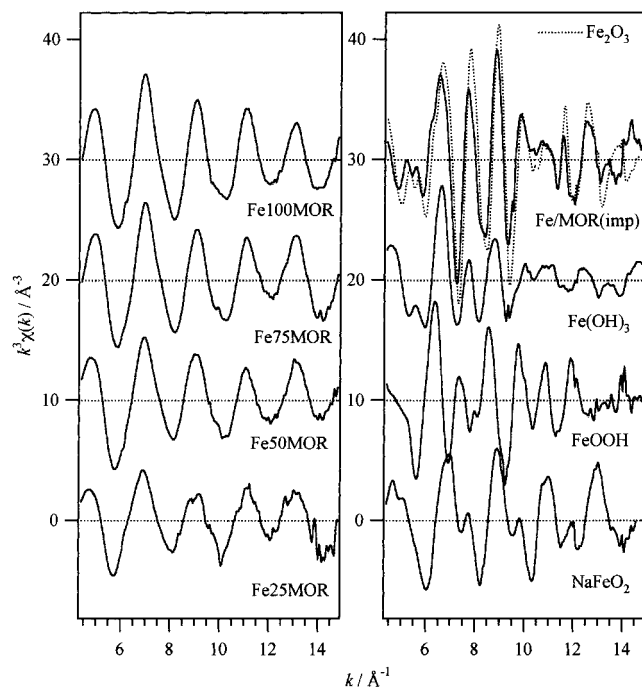

Figure 4. EXAFS oscillations of Fe-MOR (left) and Fe/MOR and reference Fe compounds (right).

Figure 5. FT-EXAFS of Fe-MOR, Fe/MOR(imp), and reference Fe compounds.

Fe−(O)−Fe scattering. The FT-EXAFS of Fe/MOR(imp) also shows several peaks, and the peaks due to Fe−Fe scattering are clearly seen at $R = 2.2-3.6$ Å. On the other hand, the FT-EXAFS of Fe-MOR samples shows almost one peak due to Fe−O scattering. For Fe-MOR samples with high Fe content (such as Fe100MOR), a small peak centered at $R = 3.1$ Å can be seen. However, the intensity of the peak is very small. It is concluded that Fe ions in Fe-MOR samples are highly dispersed onto the zeolite structure and the Fe−O−Fe bond exists in minor. If well-dispersed Fe ions exist on the mordenite structure, the Fe−O−Fe bond should rarely exist. It is suggested that the Fe−O−Fe species exist out of
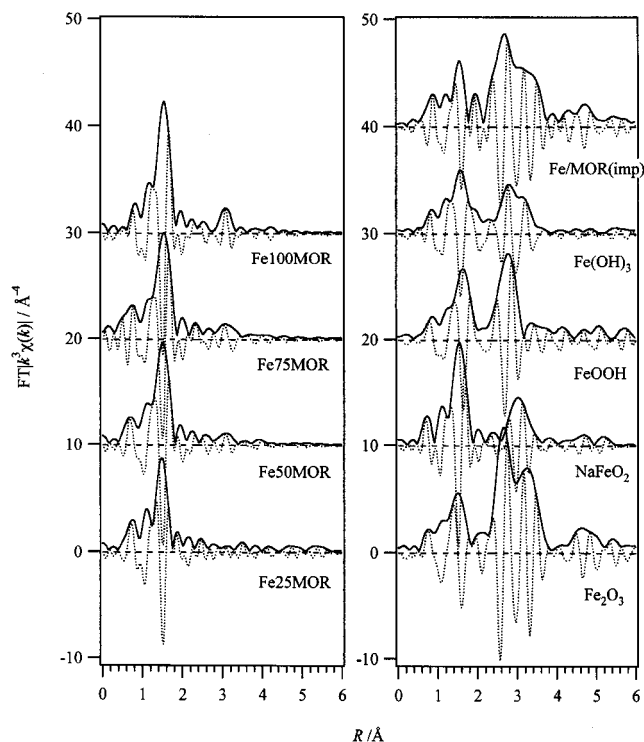
the mordenite framework. The Fe ions in Fe/MOR(imp) are formed as aggregated species, and the local structure is rather similar to that of Fe_2O_3 and/or $Fe(OH)_3$.

To obtain a detailed local structure, the curve-fitting of the Fe−O shell within $\Delta R = 1.2-1.9$ Å was performed by inverse FT after FT-filtered EXAFS in the fitting range of $\Delta k = 4-12$ Å^{-1}. In Figure 6, the best fits for Fe-MOR samples are shown as examples. In all the samples, one-shell fitting of the Fe−O shell gave satisfactory results. The parameters obtained by the EXAFS analysis of Fe-MOR are summarized in Table 3. Because of the difference of edge energy and phase shift of
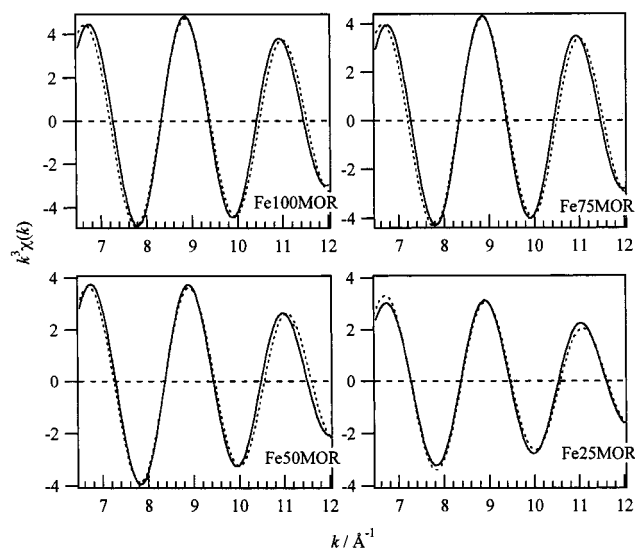
Figure 6. The best fitting of back-filtered EXAFS oscillations in the range of $\Delta R = 1.2-1.85$ Å; solid lines are the isolated EXAFS and dotted lines are the model EXAFS obtained by one-shell fitting of Fe−O.

Table 3. Evaluation of Structural Parameters Obtained by EXAFS Curve-Fitting of Fe−O Shell at $\Delta k = 1.20-1.85$ Å

sample	N	R (Å)	$\Delta\sigma^2$ (10^{-3}Å^2)	R-factor (%)
Fe25MOR	3.8	1.892	-2.37	9.9
Fe50MOR	3.9	1.895	-3.31	14.8
Fe75MOR	3.9	1.903	-4.28	14.0
Fe100MOR	4.4	1.904	-4.18	14.0

standard EXAFS of Fe−O obtained by FeAl$_2$O$_4$, large ΔE is unavoidable.

It is shown in Fe50-, Fe75- and Fe100MOR samples that the N value is almost 4. This result indicates the dominant formation of Fe−O$_4$ tetrahedra in Fe-MOR. In the case of Fe25MOR, the evaluated coordination number (N) is 3.1. It is likely that unsaturated Fe ions may coordinately coexist with Fe−O$_4$ tetrahedra. As a result, most of the substituted Fe^{3+} in Fe-MOR exist as tetrahedra in the mordenite structure. In addition, the Fe−O distance is about 1.9 Å in all the Fe-MOR samples (Table 3). It is confirmed that the completely substituted Fe-mordenite (Fe100MOR) shows low crystallinity in the mordenite structure, although tetrahedral Fe−O$_4$ structure exists. Thus, structural stability is lowered by Fe substitution with high Fe ratio. It can be suggested that the Fe ions in Fe100MOR exist in the low-crystallized mordenite species or in the amorphous ones. From these results, substituted Fe exists as Fe−O$_4$ tetrahedra in the mordenite framework in all the Fe ratio, and mordenite structure with high crystallinity and large pore volume is kept on similar to Al-MOR with the exception of Fe100MOR. In the case of Fe100MOR, the same profile of EXAFS as other Fe-MOR samples is shown although the crystallinity of the porous structure is low. It can be suggested that in all the Fe-MORs, the tetrahedral structure is formed by hydrothermal synthesis. For Fe100MOR, low crystallinity is given because of low stability of the porous framework. However, the local structure around Fe in Fe100MOR is almost similar to that in the other FeMORs. The Fe100MOR contains amorphous phases with tetrahedral Fe ions. As a result, the Fe substitution of Al brings

about tetrahedral Fe structure in Al sites, and high mordenite crystallinity can be obtained up to 75 mol % Fe. For Fe100MOR, low crystallinity is brought about because of low porous stability; it is independent of the local structure around Fe ions.

Conclusion

The Fe-substituted Al-mordenite samples with several Fe ratios were synthesized, and the local structure of Fe^{3+} ions was characterized by Al K edge XANES and Fe K edge XAFS. The points obtained in this study are summarized as follows:

(1) From the results of the N$_2$-adsorption isotherm, the Fe-substituted mordenites with Fe/(Fe + Al) ratio as high as 75 mol % have a high crystallinity and appropriate micropore. The completely substituted mordenite (Fe100MOR) shows low pore volume and crystallinity.

(2) From Al K edge XANES results, it is summarized that Fe substitution (25 mol %) of Al little affects the structural change around the Al ions. A small amount of Fe substitution does not result in a drastic effect on the structural change of the zeolite framework.

(3) The Fe K edge XAFS results indicate that the substituted Fe ions in all Fe ratios are formed as tetrahedral structures in major. The local structure around the Fe^{3+} ions is quite different from those of Fe/ MORs. The Fe−O distances are about 1.9 Å in all Fe-MOR samples. This suggests the substitution of Fe ions in Al positions in the mordenite framework.

From these insights about the detailed local Fe structure, it is concluded that Fe-substituted Al-mordenites can be obtained in a stable condition and can be expected to apply the functional material with controllable activity in catalysis. The evaluation of catalytic activity of those Fe-MORs is now in progress.